available at www.sciencedirect.com

SCIENCE DIRECT®

journal homepage: www.elsevier.com/locate/biochempharm

N-(4-Trifluoromethylphenyl)amide group of the synthetic histamine receptor agonist inhibits nicotinic acetylcholine receptor-mediated catecholamine secretion

Dong-Chan Kim [a,b], *Yong-Soo Park* [a], *Dong-Jae Jun* [a], *Eun-Mi Hur* [a], *Sun-Hee Kim* [a], *Bo-Hwa Choi* [a], *Kyong-Tai Kim* [a,*]

[a] *Division of Molecular and Life Science, SBD-NCRC, Pohang University of Science and Technology, Pohang, South Korea*
[b] *Division of Research and Development, Neuronex, Inc., San31, Hyoja-dong, Nam-gu, Pohang 790-784, South Korea*

ARTICLE INFO

Article history:
Received 1 September 2005
Accepted 23 November 2005

Keywords:
Catecholamine
DMPP
Ca^{2+} influx
Histamine-trifluoromethyltoluide
Nicotinic acetylcholine receptor
Chromaffin cells

Abbreviations:
CA, catecholamine
DMPP, 1,1-dimethyl-4-phenylpiperazinium iodide
EP, epinephrine
nAChR, nicotinic acetylcholine receptor
NA, norepinephrine
VSCC, voltage-sensitive calcium channel
VSSC, voltage-sensitive sodium channel

ABSTRACT

The therapeutic targeting of nicotinic receptors requires the identification of drugs that selectively activate or inhibit a limited range of nicotine acetylcholine receptors (nAChRs). In this study, we identified *N*-(4-trifluoromethylphenyl)amide group of the synthetic histamine receptor ligands, histamine-trifluoromethyltoluide, that act as potent inhibitors of nAChRs in bovine adrenal chromaffin cells. Catecholamine secretion induced by the nAChRs agonist, 1,1-dimethyl-4-phenylpiperazinium iodide (DMPP), was significantly inhibited by histamine-trifluoromethyltoluide. Real time carbon-fiber amperometry confirmed the ability of histamine-trifluoromethyltoluide to inhibit DMPP-induced exocytosis in single chromaffin cells. We also found that histamine-trifluoromethyltoluide inhibited DMPP-induced $[Ca^{2+}]_i$ and $[Na^+]_i$ increases, as well as DMPP-induced inward currents in the absence of extracellular calcium. Histamine-trifluoromethyltoluide had no effect on [^{3}H]nicotine binding or on calcium increases induced by high K^+, bradykinin, veratridine, histamine, and benzoylbenzoyl ATP. Among the synthetic histamine receptor ligands, clobenpropit exhibited similarity. In addition, 4′-nitroacetanilide also significantly attenuated nAChR-mediated catecholamine secretion. In conclusion, the N-(4-trifluoromethylphenyl)amide group of the histamine-trifluoromethyltoluide might be the critical moiety in the inhibition of nAChR-mediated CA secretion.

* *Corresponding author*. Present address: Department of Life Science, POSTECH, San 31, Hyoja Dong, Pohang 790-784, Republic of Korea. Tel.: +82 54 279 2297; fax: +82 54 279 2199.
E-mail address: ktk@postech.ac.kr (K.-T. Kim).
0006-2952/$ – see front matter © 2005 Elsevier Inc. All rights reserved.
doi:10.1016/j.bcp.2005.11.021

1. Introduction

Secretion of catecholamines (CAs) by the adrenal gland is elicited by stimulation with acetylcholine released from splanchnic nerve endings [1,2]. The increased permeability to Na^+, K^+ and Ca^{2+} ions through nicotinic acetylcholine receptors (nAChRs) depolarizes the chromaffin cell membrane and subsequently triggers the opening of voltage-sensitive Ca^{2+} channels (VSCCs). Extracellular Ca^{2+} influx via VSCCs subsequently induces the exocytotic fusion of chromaffin granules with the plasma membrane [3], resulting in the release of norepinephrine (NA), epinephrine (EP), ATP, and some peptides.

CAs such as dopamine, NA, and EP are synthesized in various tissues, including the brain, adrenal gland, and sympathetic ganglia, and play an important role in stress and emotional behavior [4]. In addition, CAs may also be important in affective disorders in the CNS [5,6]. Disproportion of synaptic CA levels has been implicated in various neurological diseases, including manic depressive psychosis and schizophrenia [7]. Many kinds of psychotropic drugs are known to act on CA-containing neurons [8]. Hence, physiological regulation of CA secretion is central to the understanding of the elaborate mechanism of the neuroendocrine system.

The nicotinic acetylcholine receptor (nAChR) is the paradigm of the neurotransmitter-gated ion channel superfamily [9]. The pharmacological behavior of the AChR can be described as three basic processes that progress sequentially. First, the neurotransmitter acetylcholine (ACh) binds the receptor. Next, the intrinsically coupled ion channel opens upon ACh binding with subsequent ion flux activity. Finally, the AChR becomes desensitized, a process where the ion channel becomes closed in the prolonged presence of ACh. The existing equilibrium among these physiologically relevant processes can be perturbed by the pharmacological action of different drugs. The nAChR is inhibited by a wide range of noncompetitive antagonists, including beta-amyloid1–42 peptide [10], steroids [11], and venoms [12]. Furthermore, local anesthetics, such as lidocain, procaine, and QX-222 (2-[(2,6-dimethylphenyl)amine]-*N*,*N*,*N*-triethyl-2-oxoethanaminium chloride), inhibit the function of nAChRs in a noncompetitive manner [13]. In many previous reports, the relevance between the nAChRs and antinociception have been studied [14–16]. In vitro stimulation of chromaffin cells with nAChR ligand, epibatidine evoked the release of significant levels of antinociceptive molecules [15]. Otherwise, intracerebroventricular (icv) injection of the histamine receptor agonists, histamine-trifluoromethyltoluide and imetit, produced a hypernociception in the hot plate and writhing tests [17]. Interestingly, histamine-trifluoromethyltoluide also showed non-H1 histamine receptor-mediated cellular responses [18,19]. We thus investigated the effects of synthetic histamine receptor agonists, histamine-trifluoromethyltoluide, on nAChR-mediated CA secretion in bovine adrenal chromaffin cells. We show here that N-(4-trifluoromethylphenyl)amide group of the histamine-trifluoromethyltoluide had an unusual negative effect on nAChR-mediated CA secretion in bovine adrenal chromaffin cells.

2. Materials and methods

2.1. Materials

Histamine-trifluoromethyltoluide, Dimaprit, clobenpropit, *R*-α-methylhistamine was purchased from Tocris (Bristol, UK). 2-Methylhistamine was kindly provide by Glaxosmith Kleine. Histamine, DMPP, 3′-*O*-(4-benzoyl)benzoyl ATP (BzATP), bradykinin, veratridine, 4′-nitroacetanilide and other reagents were purchased from Sigma (St. Louis, MO). Fura-2/acetoxymethylester, SBFI/acetoxymethylester, and Pluronic F-127 were obtained from Molecular Probes, Inc. (Eugene, OR). UB-165 and 5-Iodo-A-85380 were purchased from Tocris, Inc. (Ellisville, MO, USA). [^{3}H]nicotine were purchased from NEN Life Science Products (Boston, MA).

2.2. Preparation of chromaffin cells

Chromaffin cells were isolated from bovine adrenal medulla by two-step collagenase digestion as previously described [20]. For measurement of CA secretion and the [^{3}H]nicotine binding assay, cells were plated in 24-well plates at a density of 5×10^5 cells per well. Chromaffin cells transferred to 100-mm culture dishes (1×10^7 cells per dish) were used to measure cytosolic free calcium and sodium concentrations. The cells were maintained in DMEM/F-12 (Life Technologies, Inc., Grand Island, NY, USA) containing 10% bovine calf serum (HyClone, Logan, UT, USA) and 1% antibiotics (Life Technologies, Inc.). Chromaffin cells were incubated in a humidified atmosphere of 5% CO_2/95% air at 37 °C for 3–7 days before use.

2.3. $[Ca^{2+}]_i$ measurement and calcium imaging

Cytosolic free Ca^{2+} concentration ($[Ca^{2+}]_i$) was determined with the help of the fluorescent Ca^{2+} indicator fura-2 as reported previously [21]. Briefly, the chromaffin cell suspension was incubated with fresh serum-free DMEM/F-12 medium containing fura-2/AM (3 μM) for 40 min at 37 °C with continuous stirring. The cells were then washed with Locke's solution and left at room temperature until use. Sulfinpyrazone (250 μM) was added to all solutions to prevent dye leakage. Fluorescence ratios were measured by an alternative wavelength time scanning method (dual excitation at 340 and 380 nm; emission at 500 nm). For multiphoton confocal microscopic calcium imaging, chromaffin cells plated on poly-D-lysine-coated cover slips were pre-loaded with 5 μM Fluo-4 AM dye. After incubation for 30 min at 37 °C, the cells were washed two times with Locke's solution (154 mM NaCl, 5.6 mM KCl, 1.2 mM $MgCl_2$, 2.2 mM $CaCl_2$, 5 mM HEPES, and 10 mM glucose, pH 7.3) to remove excess dye and examined under the confocal microscope. Groups of chromaffin cells were selected under the microscope. Measurements of intracellular calcium were performed with the Bio-Rad Radiance 2100 confocal microscope (Bio-Rad, Inc.) equipped with a 40× objective (0.75 numerical aperture). The calcium-sensitive Fluo-4 dye was excited by the 488-nm line from a argon laser and the emission fluorescence monitored at 515/30 nm was selected by a band-pass filter. During fluorescence data collection, each scan of a 512×512 pixel image took 0.35 s, and the interval between each image scan was ~2 s.

Images were stored and processed with laser pix software (Bio-Rad, Inc.). The regions of interest (ROIs) distributed across the image provided an intensity versus time graphic output.

2.4. Amperometric measurement

Electrophysiological recording conditions were as we described previously [21]. Briefly, recordings were performed at room temperature in amine-free solution containing 137.5 mM NaCl, 2.5 mM KCl, 2 mM $CaCl_2$, 1 mM $MgCl_2$, 10 mM D-glucose, and 10 mM HEPES, pH 7.3 with NaOH. Carbon-fiber electrodes were fabricated from 5 to 11 μm carbon-fibers (PAN T650 or P25; Amoco performance Products) and polypropylene 10 μl micropipettor tips as described by Koh and Hille [22]. A carbon-fiber electrode, backfilled with 3.5 M KCl to connect to the headstage, was attached to a single cell. The amperometric current was measured using an Axopatch 200B amplifier (Axon Instruments, Inc., CA) and operated in the voltage-clamp mode at a holding potential of +600 mV. Amperometric signals were low-pass filtered at 1 kHz, then sampled at 0.5 kHz. For data acquisition and analysis, pClamp 8 software (Axon Instruments, Inc., CA) and IGOR software (WaveMetrics, OR) were used. Solutions were exchanged by a local perfusion system that allows complete exchange of medium bathing the cells within 2 s.

2.5. Measurement of CA secretion by HPLC

CA secretion from chromaffin cells was measured in 24-well plates following the method reported previously [21]. In brief, cells were rinsed two times with Ca^{2+}-containing Locke's solution and were incubated at 37 °C for 5 min in each case. The cells were subsequently stimulated with the drugs under test. After the incubation, the medium was removed from each well and transferred to a test tube containing (10%, v/v) 0.1N HCl. A 20 μl aliquot of each sample was injected onto the HPLC (BAS 480, BioAnalytical System, Inc., IN, USA) C18 column (150 mm × 1 mm) with electrochemical detection. The potential used was +770 mV versus Ag/AgCl, with a classic 3 mm glassy carbon electrode. The ranges of sensitivity for the electrode were 100 and 50 nA with a flow rate of 1 ml/min. The 2 l of mobile phase included: 0.55 g heptanesulfonic acid, 0.2 g EDTA, 80 ml acetonitrile, 12 ml 85% phosphoric acid, 16 ml triethylamine with the pH adjusted to 2.5 with H_3PO_4 and filtered with 0.45 micron membrane. Stock catecholamine (NA, EP, DA) solutions were used as standards.

2.6. Measurement of intracellular Na^+ level

Cytosolic free Na^+ concentration ($[Na^+]_i$) was measured using the fluorescent Na^+ indicator SBFI as previously described [21]. In brief, the chromaffin cell suspension was incubated in fresh DMEM/F-12 medium containing 15 μM SBFI/AM, 10% bovine calf serum, and 0.2% Pluronic F-127 for 2 hr at 37 °C with continuous stirring. The cells were then washed twice with fresh DMEM/F-12 medium and left at room temperature until use. Sulfinpyrazone (250 μM) was added to all solutions to prevent dye leakage. Before measurement, a small aliquot of the cells (1×10^6 cells) was taken for assay, centrifuged, and resuspended in Locke's solution after the supernatant was removed. Fluorescence ratios were measured with alternate excitation at 340 and 380 nm and emission at 530 nm. Because the calibrations of the obtained fluorescence ratios for Na^+ concentrations are not absolute, we expressed our results as fluorescence ratios.

2.7. Electrophysiological recording

Whole-cell patch clamp recordings were performed to measure inward sodium current through nAChRs with an Axopatch 200B amplifier (Axon Instruments, Foster City, CA) and Digidata 1200 interface. Isolated chromaffin cells were plated on poly-D-lysine-coated glass chips and incubated for 2–3 days at 37 °C in 5% CO_2. The pipettes were fire-polished and had a typical resistance of 5–6 MΩ. The bath solution contained 137.5 mM NaCl, 2.5 mM KCl, 2 mM $CaCl_2$, 1 mM $MgCl_2$, 10 mM glucose, and 10 mM HEPES titrated to pH 7.3 with NaOH. The intracellular solution contained 140 mM CsCl, 3 mM EGTA, 1 mM $MgCl_2$, and 10 mM HEPES titrated to pH 7.3 with CsOH. Currents were filtered at 1 kHz, and then sampled at 5 kHz. Step pulses were applied from 0 to −120 mV for 360 ms with an interpulse interval of 1 s and voltage ramp was performed from −120 to +50 mV for 250 ms to show voltage–current relationship of nAChRs. For data acquisition and analysis, pClamp 8 software (Axon instruments, Foster City, CA) was used. Solutions were exchanged by a local perfusion system that allows complete exchange of medium bathing the cells within 2 s. Values are presented as mean ± S.E.M.

2.8. Inhibition of [^{3}H]nicotine binding

Binding of [^{3}H]nicotine to intact cells was measured as previously described [21]. Intact chromaffin cells in 24-well plates (5×10^5 cells/well) were washed twice with Locke's solution and incubated with 40 nM [^{3}H]nicotine and the indicated concentrations of drug for 40 min at 25 °C. Then, the cells were washed three times with 1 ml ice-cold Ca^{2+}-free Locke's solution containing 100 μM EGTA. Finally, the cells were lysed by being scraped into 0.5 ml 5% trichloroacetic acid, and the radioactivity was measured by liquid scintillation counting. Nonspecific binding, determined by co-incubation with 1 mM nicotine, amounted to less than 20% of total binding, and was routinely subtracted from the total binding. The binding data were analyzed and expressed as percentage of specific binding.

2.9. Mn^{2+} quenching of fura-2 fluorescence

The Mn^{2+} quenching assay was performed as described by Choi et al. [23]. Briefly, fura-2-loaded cells (5×10^6 cells/ml; described above) were placed into a quartz cuvette in a thermostatically controlled cell holder at 37 °C under continuous stirring. Fluorescence was excited at 360 nm, i.e., the isosbestic wavelength at which Ca^{2+} does not affect fura-2 fluorescence and at which, therefore, changes are caused by Mn^{2+} quenching. Emission was recorded at 500 nm. The potency and slope of the change in fluorescence intensity were recorded after applying 2 mM $MnCl_2$ and the drugs to be tested.

2.10. Statistical analysis

All experiments were independently repeated a minimum of three times. All traces presented are representative of more than three separate experiments. All quantitative data are presented as means ± S.E.M. Comparisons between two groups were analyzed via Student's *t*-test, and values of $P < 0.05$ were considered to be significant. IC_{50} values were calculated with the MicroCal Origin for Window program.

3. Results

3.1. Inhibitory effect of histamine-trifluoromethyltoluide on nAChR-mediated exocytosis

To study the effect of histamine-trifluoromethyltoluide (Fig. 1A) on DMPP-evoked CA secretion, we treated chromaffin cells with 1–100 μM histamine-trifluoromethyltoluide and quantitated CA secretion by HPLC. By itself, histamine-trifluoromethyltoluide did not induce CA secretion (data not shown). When histamine-trifluoromethyltoluide was applied 1 min before DMPP stimulation, CA secretion was significantly reduced ($IC_{50} = 3.2 \pm 0.8$ μM) compared with the amount induced by DMPP alone (Fig. 2A). Histamine-trifluoromethyltoluide, however, had no effect on CA secretion induced by 60 mM KCl (Fig. 2A). To better understand how histamine-trifluoromethyltoluide inhibits the secretory response evoked by nicotinic stimulation, we measured exocytosis from single bovine adrenal chromaffin cells using the amperometric method. When a brief pulse (20 s) of DMPP was applied to a single chromaffin cell, a fast and transient increase in current occurred (Fig. 2B). When cells were subjected to repetitive stimulation with DMPP (up to four times for 20 s each and at 2 min

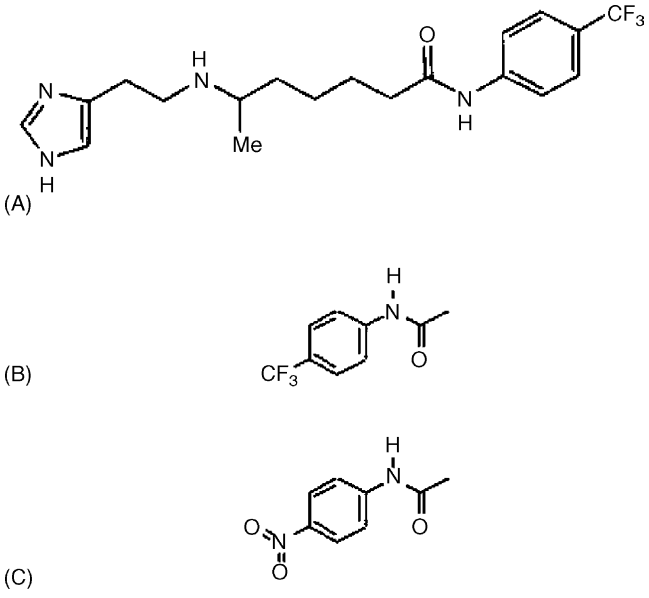

Fig. 1 – Chemical structures of histamine-trifluoromethyltoluide (A), *N*-(4-trifluoromethylphenyl)amide group of histamine-trifluoromethyltoluide (B), and 4′-nitroacetanilide (C).

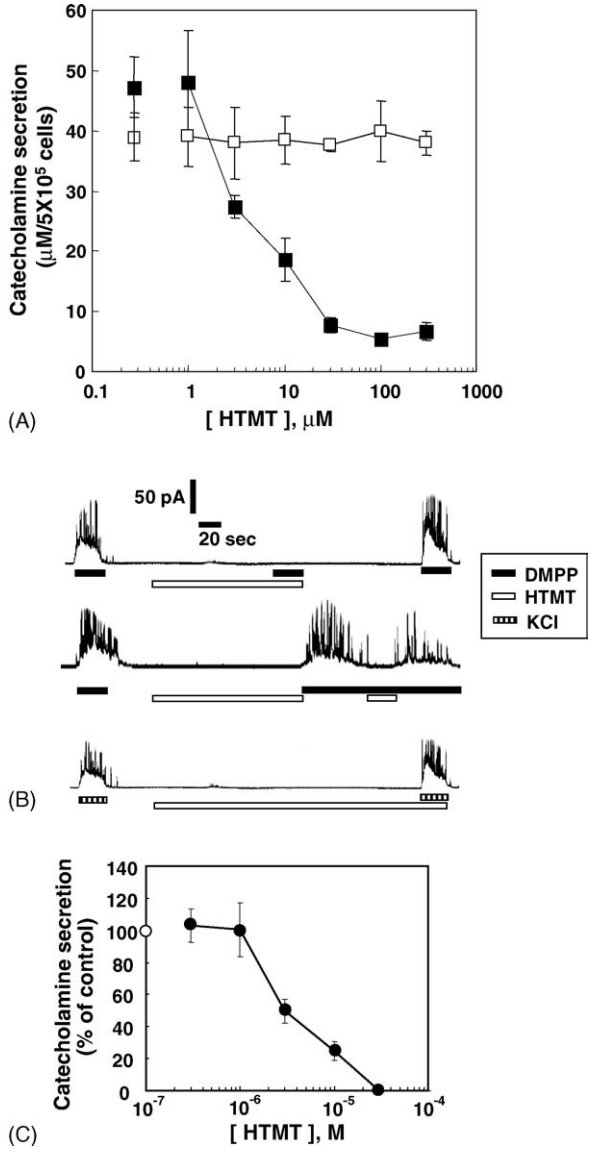

Fig. 2 – Inhibitory effect of histamine-trifluoromethyltoluide (HTMT) on CA in bovine chromaffin cells. (A) Bovine chromaffin cells were treated with 10 μM DMPP (closed box) or 60 mM KCl (open box) in the presence of the various concentration of HTMT for 10 min. The secreted CA were measured by HPLC as described in Section 2. The experiments were performed three times independently, and the results were reproducible. Data were the means ± S.E.M. ($n = 3$) values. (B) Inhibitory effect on catecholamine secretion in single bovine chromaffin cell. Chromaffin cells were stimulated with 10 μM DMPP, or 60 mM KCl for 20 s in the absence or presence of 30 μM HTMT, respectively. (C) Total amperometric currents induced by the 20 s DMPP pulse were integrated and represented as percentage of the average currents by DMPP pulses without (open circle) or with various concentration of HTMT (closed circle). The experiments were performed three times independently, and the results were reproducible. Data were the means ± S.E.M. ($n = 8$) values.

intervals), a similar amount of exocytosis was observed in response to each stimulation, without significant rundown (data not shown). While histamine-trifluoromethyltoluide did not inhibit exocytosis induced by 60 mM KCl (Fig. 2B), the presence of histamine-trifluoromethyltoluide 100 s before and during the 20 s DMPP pulse reduced CA secretion in a concentration-dependent manner ($IC_{50} = 2.9 \pm 0.6$ μM) (Fig. 2C). The effect of histamine-trifluoromethyltoluide was partially reversible immediately after its removal and completely reversible 2 min after its removal. These results clearly indicate that histamine-trifluoromethyltoluide inhibits nAChR-mediated exocytosis in chromaffin cells.

3.2. *Inhibitory effects of histamine-trifluoromethyltoluide on nAChR-mediated calcium increases*

Since an increase in $[Ca^{2+}]_i$ is an essential step in CA secretion, we investigated the effect of histamine-trifluoromethyltoluide on DMPP-induced calcium increase. Histamine-trifluoromethyltoluide alone, at concentrations up to 300 μM, had no effect on $[Ca^{2+}]_i$ (data not shown), whereas the DMPP-induced increase in $[Ca^{2+}]_i$ (Fig. 3A, trace 'a') was inhibited by histamine-trifluoromethyltoluide (Fig. 3A, trace 'b') in a concentration-dependent manner and with an IC_{50} of 5.7 ± 0.3 μM (Fig. 3B). At a concentration of 30 μM, histamine-trifluoromethyltoluide completely inhibited the DMPP-induced calcium increase. Histamine-trifluoromethyltoluide also inhibited the $[Ca^{2+}]_i$ increase induced by nicotine to a similar extent (data not shown).

To obtain further information about the mechanism of action of histamine-trifluoromethyltoluide, we assayed the time course of its effect on the DMPP-induced calcium increase. When chromaffin cells were treated simultaneously with DMPP and 10 μM histamine-trifluoromethyltoluide, the initial peak height was decreased by 74% compared with that observed with DMPP. The effect of histamine-trifluoromethyltoluide was similar regardless of incubation time (Fig. 3C), indicating that histamine-trifluoromethyltoluide acts very rapidly, and suggesting that this compound acts directly on nAChRs in the plasma membrane rather than via the generation of second messengers. We therefore tested the effects of different concentrations of DMPP in the presence of 10 μM histamine-trifluoromethyltoluide. We found that the effect of DMPP on $[Ca^{2+}]_i$ increases were concentration dependent, reaching a maximum at 30 μM (Fig. 3D, open boxes), and that histamine-trifluoromethyltoluide inhibited this DMPP-induced $[Ca^{2+}]_i$ increase to a similar extent at all DMPP concentrations tested (Fig. 3D, closed boxes), indicating that histamine-trifluoromethyltoluide does not act in a competitive manner. We also

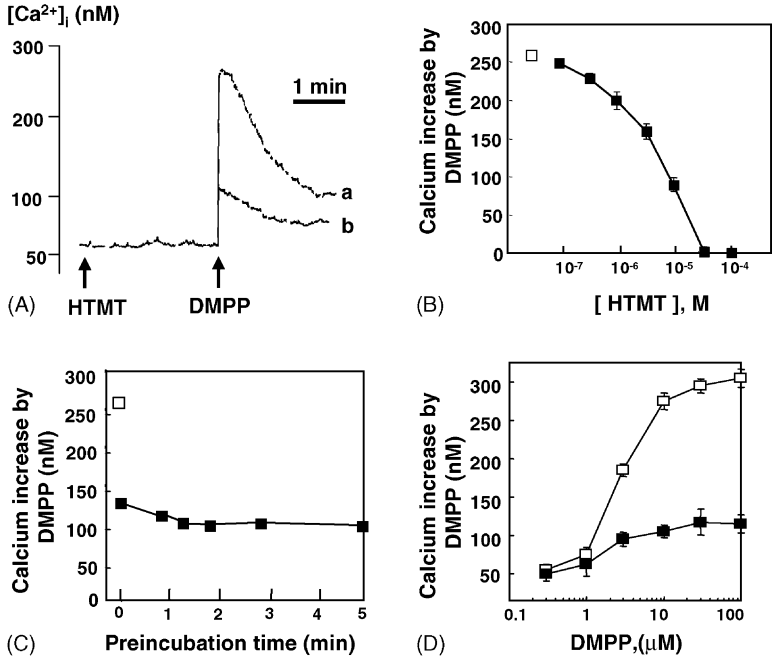

Fig. 3 – Inhibitory effect of HTMT on $[Ca^{2+}]_i$ elevation in chromaffin cells. (A) The intracellular $[Ca^{2+}]_i$ rise induced by 10 μM DMPP was measured in the absence (trace a) or presence (trace b) of 10 μM HTMT. Cells were incubated with HTMT for 3 min before stimulation with DMPP. The experiments were performed three times independently and the typical Ca^{2+} traces are presented. (B) The calcium increase induced by 10 μM DMPP was measured 3 min after preincubation with the indicated concentrations of HTMT (closed box). The peak height of each stimulation was compared to that of the control calcium increase caused by DMPP alone (open box). Data are the means ± S.E.M. (bars) values of triplicate measurements. (C) Chromaffin cells were preincubated for the indicated times with 30 μM HTMT and then stimulated with 10 μM DMPP (closed box). Incubation with zero time indicates simultaneous treatment with both HTMT and DMPP. The peak height of each stimulation was compared to that of the control calcium increase caused by DMPP alone (open box). (D) The calcium increase induced by the indicated concentrations of DMPP was measured in the absence (open box) or presence (closed box) of 10 μM HTMT. Data are the means ± S.E.M. (bars) values of triplicate measurements.

monitored $[Ca^{2+}]_i$ increases in single chromaffin cells using confocal microscopic calcium imaging (Fig. 4). When cells were treated with 30 μM histamine-trifluoromethyltoluide for 5 min, the fluorescence intensity in response to 10 μM DMPP was markedly reduced (Fig. 4A). In contrast, histamine-trifluoromethyltoluide had no effect on KCl-evoked calcium entry (Fig. 4B).

3.3. *Inhibitory effect of histamine-trifluoromethyltoluide on sodium influx through nAChR*

Since both calcium channels and nAChRs are activated by nicotinic stimulation [21], the inhibition of DMPP-induced $[Ca^{2+}]_i$ increase by histamine-trifluoromethyltoluide may result from inhibition of either of these channels. To verify

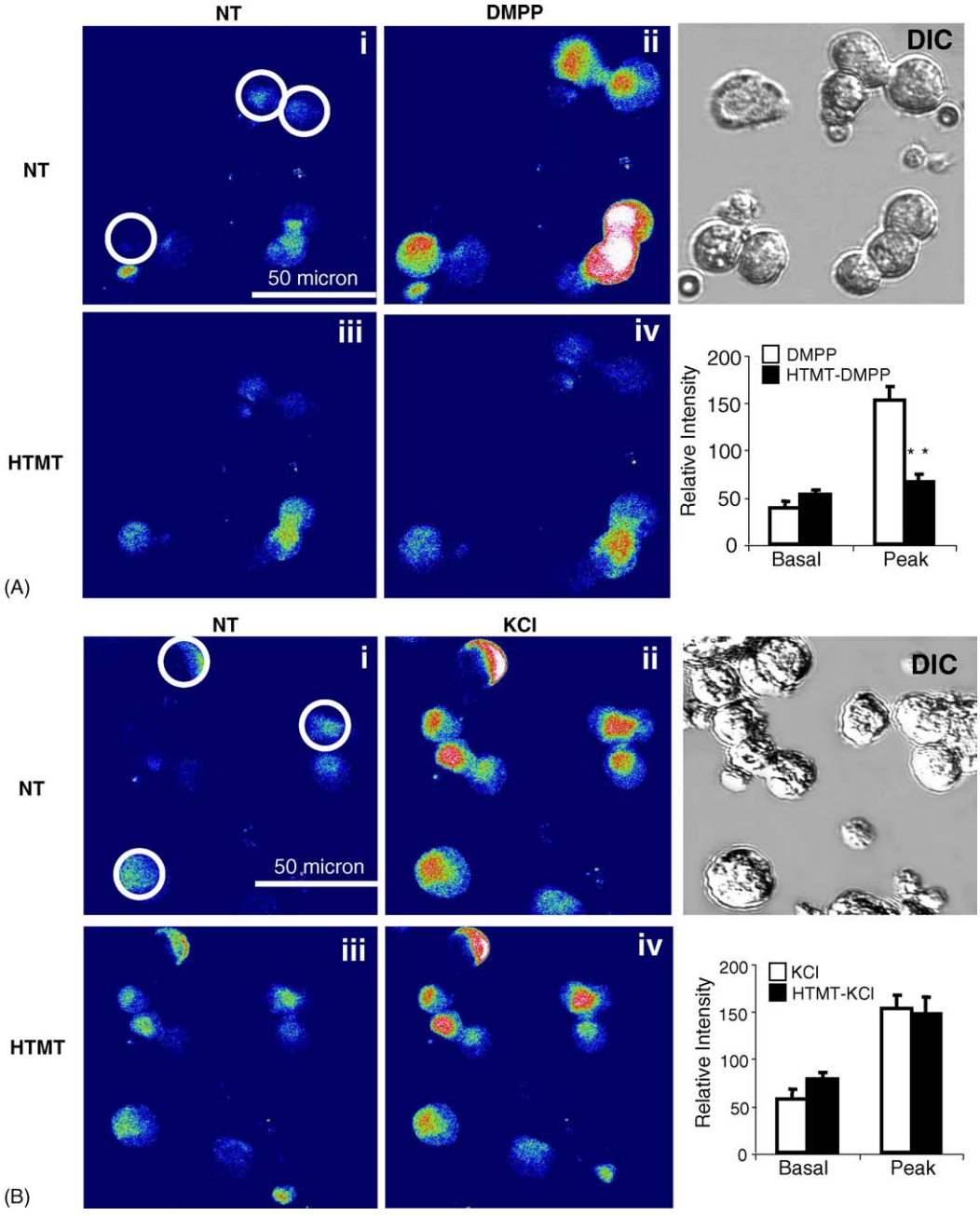

Fig. 4 – Inhibitory effect of HTMT in $[Ca^{2+}]_i$ elevation in bovine chromaffin cells. The intracellular $[Ca^{2+}]_i$ rise induced by 10 μM DMPP (A) or 60 mM KCl (B) was measured via multiphoton confocal microscope using calcium sensitive dye Fluo-4 AM. Cells were stimulated by 10 μM DMPP or 60 mM KCl in the absence (ii) or presence (iv, 5 min preincubation) of 30 μM HTMT. Left lower pictures (iii) were conditioned by 30 μM HTMT alone. In the bar graphs of each panel, filled bars represented induction by DMPP or KCl alone (i and ii), and open bars induction by each stimulants in the 5 min preincubation of 30 μM HTMT (iii and iv), respectively. The experiments were performed three times independently, and the results were reproducible. Typical sets of pictures were presented. Significant differences between DMPP alone and DMPP + HTMT are presented. $^{**}P < 0.01$. Values were represented average fluorescence intensity (ROI) ± S.E.M. in selected circled three areas.

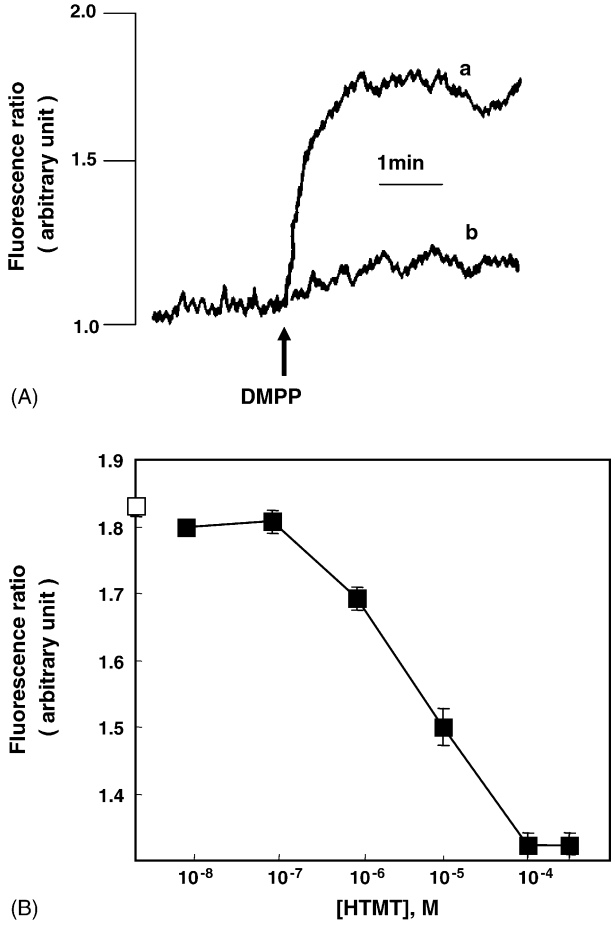

Fig. 5 – Inhibitory effect of HTMT on sodium increase in bovine chromaffin cells. (A) The intracellular sodium increase induced by 10 μM DMPP was measured in the absence (trace a) or presence (trace b) of 30 μM HTMT. The experiments were performed three times independently, and the results were reproducible. Typical Na^+ traces were presented. (B) The sodium increase induced by 10 μM DMPP was measured 5 min after preincubation with the indicated concentration of HTMT (closed boxes). The peak height of each stimulation was compared to that of the control sodium increase caused by DMPP alone (open box). Data are the means ± S.E.M. (bars) values of triplicate measurements.

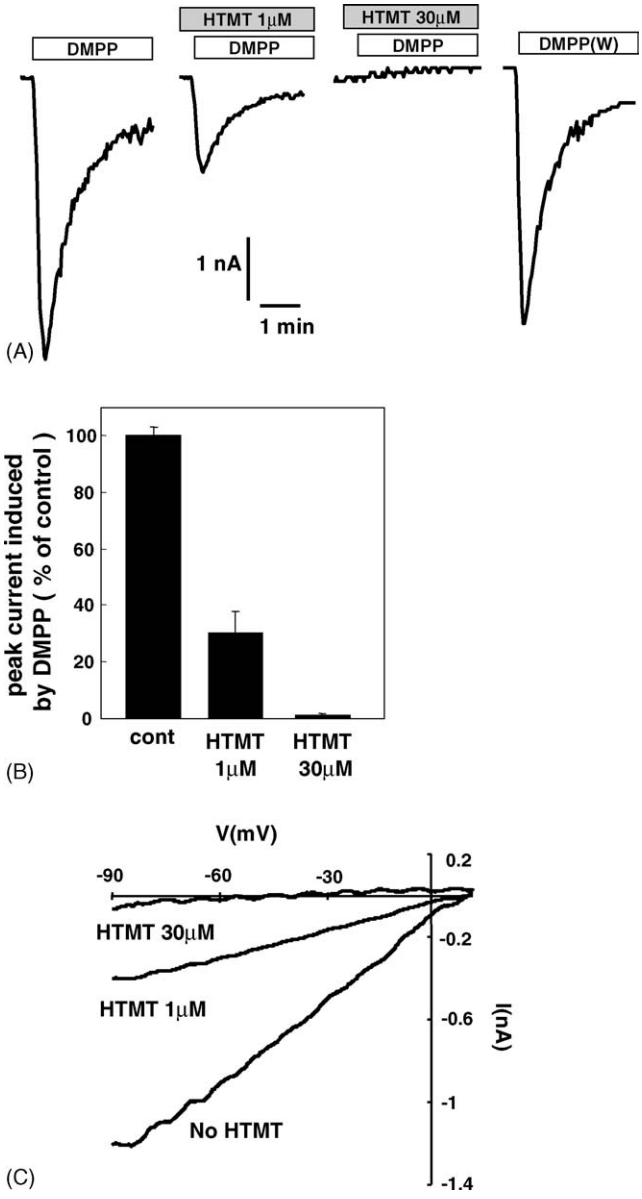

Fig. 6 – (A) The intracellular sodium current induced by 10 μM DMPP was recorded through whole-cell patch clamp in the absence or presence of indicated HTMT concentrations. Inductions by DMPP were performed after the 5 min preincubation of HTMT and washed out for 3 min to get back the control response. (B) Total peak currents induced by DMPP were integrated and represented as percentage of average currents by DMPP. Data were the means ± S.E.M. (n = 6) values. (C) The traces by voltage ramp application from −120 to +50 mV were presented in each case of DMPP stimulation with or without HTMT.

directly whether nAChRs are inhibited by histamine-trifluoromethyltoluide, we tested its effects on DMPP-induced sodium increase, which occurs only through nAChRs. We found that the DMPP-induced increase in cytosolic sodium (Fig. 5A) was inhibited by histamine-trifluoromethyltoluide in a concentration-dependent manner with an IC_{50} of 6.1 ± 1.2 μM (Fig. 5B), with complete inhibition at 100 μM histamine-trifluoromethyltoluide (Fig. 5A, trace b). These results suggest that the histamine-trifluoromethyltoluide inhibition of DMPP-induced calcium and sodium increases resulted from its direct inhibition of nAChRs. To more clearly assess the effects of histamine-trifluoromethyltoluide on sodium influx through nAChRs, we performed whole-cell patch clamp experiments to observe the nAChR-mediated sodium current. We found that DMPP elicited an inward current, which, in the continuous presence of DMPP, declined after reaching a peak (Fig. 6A). In the presence of 1 μM histamine-trifluoromethyltoluide, however, the nicotinic current declined to 30.3 ± 2.7% of the control (Fig. 6B). The nAChR-mediated current–voltage relationship in the absence or

presence of histamine-trifluoromethyltoluide was determined by applying a ramp pulse from −120 to +50 mV for 250 ms at the time of the peak. We observed no apparent shift in the voltage dependence of the current in response to histamine-trifluoromethyltoluide (Fig. 6C). The inhibitory effects of the histamine-trifluoromethyltoluide were often reversible, although it took as long as 20 min to completely wash out the histamine-trifluoromethyltoluide (Fig. 6A; DMPP(W)).

3.4. *Lack of histamine-trifluoromethyltoluide effect on nicotine binding*

Since the inhibitory effect of histamine-trifluoromethyltoluide is almost instantaneous and specific for nAChR, we thought it likely that histamine-trifluoromethyltoluide directly binds to nAChRs. When we tested whether histamine-trifluoromethyltoluide inhibits the binding of [^{3}H]nicotine to nAChRs, we found that histamine-trifluoromethyltoluide did not significantly compete for binding with [^{3}H]nicotine (Fig. 7), suggesting that its binding site is distinct from that of the receptor agonists, including nicotine and acetylcholine.

3.5. *Receptor specificity of histamine-trifluoromethyltoluide*

We determined the specificity of histamine-trifluoromethyltoluide-induced inhibitory effects by testing its effects on calcium channels, sodium channels, and phospholipase C (PLC)-linked receptor signaling. We first test the inhibitory effect of histamine-trifluoromethyltoluide on the nicotine-induced calcium increase. Histamine-trifluoromethyltoluide significantly reduced nicotine-induced calcium increase in concentration-dependent manner (Fig. 8A and B). We also found that the increase in calcium induced by 60 mM K^+ was not inhibited by pretreatment with 10 μM histamine-trifluoromethyltoluide, suggesting that voltage-dependent calcium channels are not affected by histamine-trifluoromethyltoluide (Fig. 8). In bovine adrenal chromaffin cells, veratridine-induced activation of sodium channels is known to cause membrane depolarization [24,25], thereby leading to a slow and weak increase in calcium through voltage-sensitive calcium channels [26]. We found that histamine-trifluoromethyltoluide had no effect on this veratridine-induced calcium increase (Fig. 8). Bradykinin and histamine have been found to activate PLC-linked B2 bradykinin and H_1 histamine receptors, respectively, in bovine adrenal chromaffin cells [21,27]. We found that histamine-trifluoromethyltoluide had no effect on the increases in calcium induced bradykinin or histamine (Fig. 8). Secretion of CAs by rat PC12 pheochromocytoma cells is strongly stimulated by extracellular ATP via P2-type purinergic receptors [28,29]. Since benzoylbenzoyl ATP (BzATP), an ATP analogue, has been found to cause a concentration- and time-dependent Ca^{2+} influx via P2X2 receptors in PC12 cells [30], we pretreated these cells with histamine-trifluoromethyltoluide to determine if it had any effect on BzATP-induced Ca^{2+} influx. We found that histamine-trifluoromethyltoluide did not affect P2X2 activities (Fig. 8).

Taken together, these results indicate that histamine-trifluoromethyltoluide has no significant inhibitory effect on calcium channels, sodium channels, and PLC-linked B2 or H_1 receptors. Thus, these findings indicate that the effect of \histamine-trifluoromethyltoluide on nAChRs is highly specific.

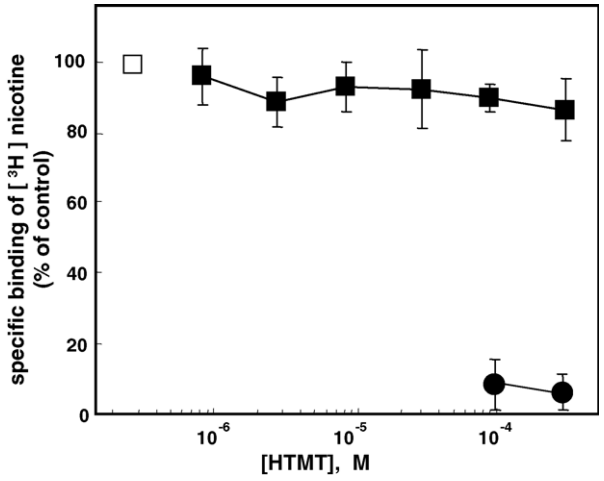

Fig. 7 – Effect of HTMT on [^{3}H]nicotine binding. Chromaffin cells were incubated with 40 nM [^{3}H] nicotine and various concentrations of HTMT (closed box) for 40 min at 25 °C. Specific binding of [^{3}H]nicotine was presented. Total binding was presented by open box. Nonspecific binding was determined in the presence of 1 mM unlabeled nicotine (closed circle). The experiments were performed three times independently, and the results were reproducible. Data were the means ± S.E.M. (n = 3) values.

3.6. *Effects of histamine-trifluoromethyltoluide on nAChR subtypes*

To determine whether histamine-trifluoromethyltoluide is specific for any nAChR subtype, we tested its effects on intracellular calcium induced by the selective α4β2 and α3β2 agonists, 5-Iodo-A-85380 [31] and UB-165 [32], respectively (Fig. 9). We found that UB-165-induced a greater increase in intracellular calcium than A-85380 (Fig. 9A), suggesting that α3β2 type nAChRs are more highly expressed than α4β2 types in bovine adrenal chromaffin cells. We found that histamine-trifluoromethyltoluide inhibited the calcium increase induced by both nAChR selective agonists, and to a similar extent (Fig. 9B).

3.7. *Comparison between histamine-trifluoromethyltoluide and other synthetic histamine receptor ligands*

Histamine-trifluoromethyltoluide is a synthetic histamine derivative containing its side chain amide group with trifluoromethylphenyl heptanecarboxamide. We compared the effect of histamine-trifluoromethyltoluide with that of other histamine derivatives. Similar to histamine-trifluoromethyltoluide, clobenpropit, a synthetic H_4 histamine receptor agonist, attenuated the DMPP-induced calcium increase (Fig. 10). In contrast, we could not observe any effects with 2-methylhistamine as an H_1 receptor agonist, dimaprit as an

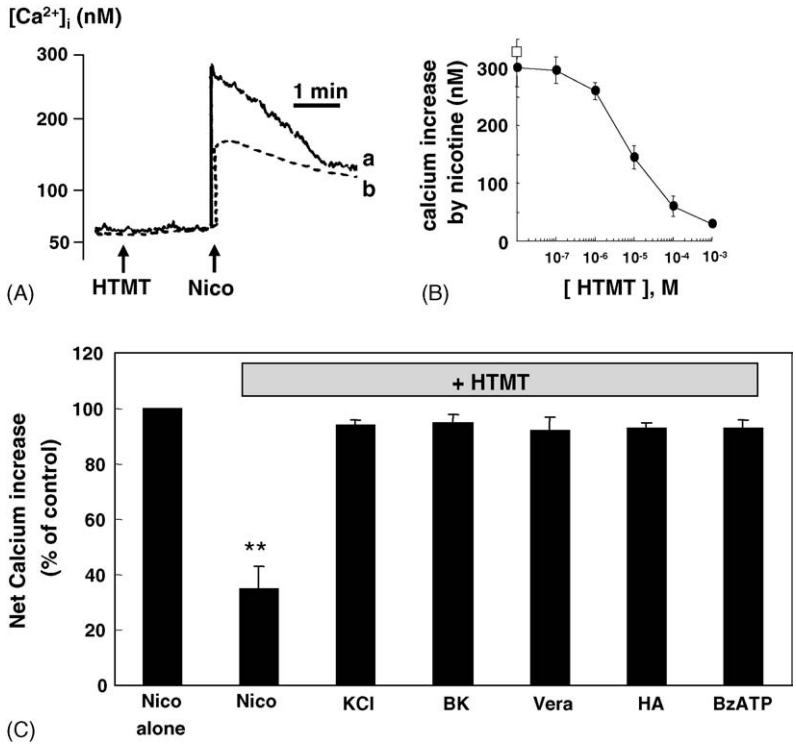

Fig. 8 – Specificity of HTMT action. (A) The intracellular $[Ca^{2+}]_i$ rise induced by 10 μM nicotine (Nico) was measured in the absence (trace a) or presence (trace b) of 5 μM HTMT. Cells were incubated with HTMT for 3 min before stimulation with nicotine. The experiments were performed three times independently and the typical Ca^{2+} traces are presented. (B) The calcium increase induced by 10 μM nicotine was measured 3 min after preincubation with the indicated concentrations of HTMT (closed circle). The peak height of each stimulation was compared to that of the control calcium increase caused by nicotine alone (open box). Data are the means ± S.E.M. (bars) values of triplicate measurements. (C) Lack of HTMT effect on the rise in $[Ca^{2+}]_i$ induced by high K^+, bradykinin, histamine, veratridine, and BzATP. The intracellular $[Ca^{2+}]_i$ increase was induced by 60 mM KCl (K^+), 10 μM nicotine (Nico), 5 μM bradykinin (BK), 100 μM histamine (HA), 200 μM veratridine (Vera), and 300 μM BzATP in the presence of 10 μM HTMT. Significant differences between nicotine alone and nicotine + HTMT are presented. $^*P < 0.05$. The results were reproducible. Data were the means ± S.E.M. ($n = 3$) values.

H_2 receptor agonist, or *R*-α-methylhistamine as an H_3 receptor agonist (Fig. 10A). The ability of histamine-trifluoromethyltoluide to block nAChRs was unrelated to the histamine group (Fig. 8). Since the histamine-trifluoromethyltoluide purchased from TOCRIS is a di-maleate salt, we tested the contribution of the latter moiety (di-maleate salt) to the effects of histamine-trifluoromethyltoluide. We found that di-maleate salt did not have any effect (data not shown).

In addition to blocking the DMPP-induced Ca^{2+} increase, clobenpropit also blocked DMPP-induced CA secretion (Fig. 10C) and Na^+ current (data not shown), similar to our findings with histamine-trifluoromethyltoluide. We also tested the effects of histamine-trifluoromethyltoluide and clobenproprit and found that they inhibit Ca^{2+} influx upon nicotinic stimulation. In fura-2-loaded cells, DMPP stimulation accelerated fura-2 fluorescence quenching in the presence of extracellular Mn^{2+}. Treatment with histamine-trifluoromethyltoluide (Fig. 10B, trace b) and clobenpropit (Fig. 10B, trace d) dramatically reduced the rate of fluorescence quenching caused by DMPP. Since the structure of 4′-nitroacetanilide (Fig. 1B) and *N*-(4-trifluoromethylphenyl)-amide group of histamine-trifluoromethyltoluide (Fig. 1A) are very similar, we compared the inhibitory effects of histamine-trifluoromethyltoluide, clobenpropit, and 4′-nitroacetanilide on DMPP-induced CA secretion. All three compounds significantly blocked DMPP-induced CA secretion, with clobenpropit having the most potent effect (Fig. 10C), indicating that the *N*-(4-trifluoromethylphenyl)amide group is the critical structural part of these molecules involved in the inhibition of nAChR-mediated Ca^{2+} influx and CA secretion.

4. Discussion

We have shown here that one of the the synthetic histamine receptor ligands, histamine-trifluoromethyltoluide, selectively inhibits nAChRs, thereby causing reduction of CA secretion from bovine adrenal chromaffin cells. Histamine-trifluoromethyltoluide inhibited all the DMPP-induced responses tested, including CA secretion and $[Ca^{2+}]_i$ and $[Na^+]_i$ increases, thus indicating that histamine-trifluoromethyltoluide selectively suppresses nAChRs activity, as well as inhibiting nicotine-induced responses. In contrast, the increases in $[Ca^{2+}]_i$ induced by high K^+, veratridine, BzATP and

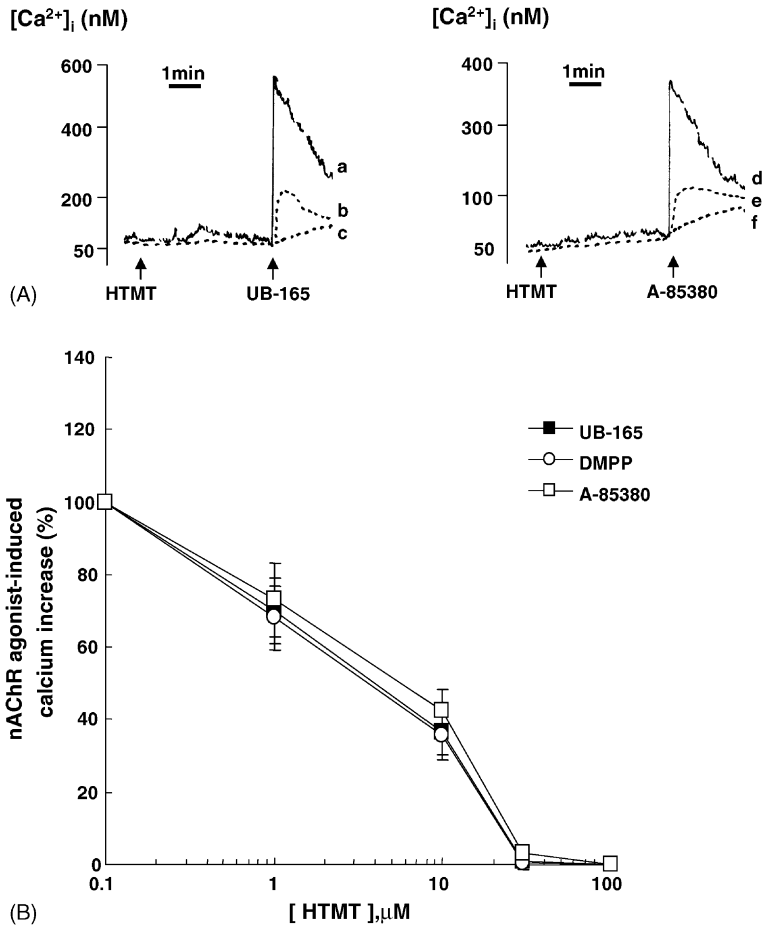

Fig. 9 – Comparison of the inhibitory effects of HTMT on calcium increase by nAChR subtype selective agonists. (A) The intracellular $[Ca^{2+}]_i$ rise induced by subtype selective nAChR agonists was measured in the absence (trace a), presence of 10 μM HTMT (trace b) or 30 μM HTMT (trace c). Cells were incubated with HTMT for 3 min before stimulation with UB-165 or A-85380. The experiments were performed three times independently and the typical Ca^{2+} traces are presented. (B) The induction of calcium by 10 μM DMPP (open circle), 1 μM UB-165 (closed box), and 1 μM 5-Iodo A-85380 (open box) for α3β2 and α4β2 subtype, respectively, was inhibited by 3 min pretreatment of HTMT with indicated concentration. Data are the means ± S.E.M. (bars) values of triplicate measurements.

bradykinin were not affected by histamine-trifluoromethyltoluide, suggesting that histamine-trifluoromethyltoluide has no effect on voltage-sensitive calcium channels (VSCCs), voltage-sensitive sodium channels (VSSCs), P2X receptors, and PLC-linked receptors. Moreover, histamine-trifluoromethyltoluide itself did not induce an increase in $[Ca^{2+}]_i$, nor did it affect the histamine-mediated calcium increase, suggesting that it does not act on H_1Rs even though it is a potent H_1R agonist. Although VSCCs are stimulated during the activation process of nAChRs, the inhibition by histamine-trifluoromethyltoluide of DMPP-induced sodium increases and its inability to inhibit high K^+-induced calcium increases clearly indicate that nAChRs, not calcium channels, are the specific target of histamine-trifluoromethyltoluide. Moreover, the inability of histamine-trifluoromethyltoluide to block [^{3}H] nicotine binding indicates that histamine-trifluoromethyltoluide acts as a noncompetitive nAChR inhibitor.

At present, histamine-trifluoromethyltoluide is the only commercially available H_1R agonist [17,33,34], which was shown to induce $[Ca^{2+}]_i$ in promyelocytes [34]. We have shown here, however, that histamine-trifluoromethyltoluide itself did not induce $[Ca^{2+}]_i$ in bovine adrenal chromaffin cells nor did it inhibit H_1R-mediated calcium responses. The differences between these findings may be due to differences in the specific residues that interact with the agonist, since the conformation of H_1R varies with cell type. Thus, the structural features of histamine-trifluoromethyltoluide involved in its interaction with nAChR are important. As we mentioned above, histamine-trifluoromethyltoluide is a synthetic histamine derivative [35] containing its side chain amide group with trifluoromethylphenyl heptanecarboxamide. To show whether the activity against nAChRs is due to the trifluoromethylphenyl heptanecarboxamide or the histamine group, we pretreated cells with histamine and then activated the nAChRs with DMPP (Fig. 8C). Histamine, however, had no effect on the DMPP-induced Ca^{2+} elevation. These results suggest that the trifluoromethylphenyl heptanecarboxamide group of the histamine-trifluoromethyltoluide may be the

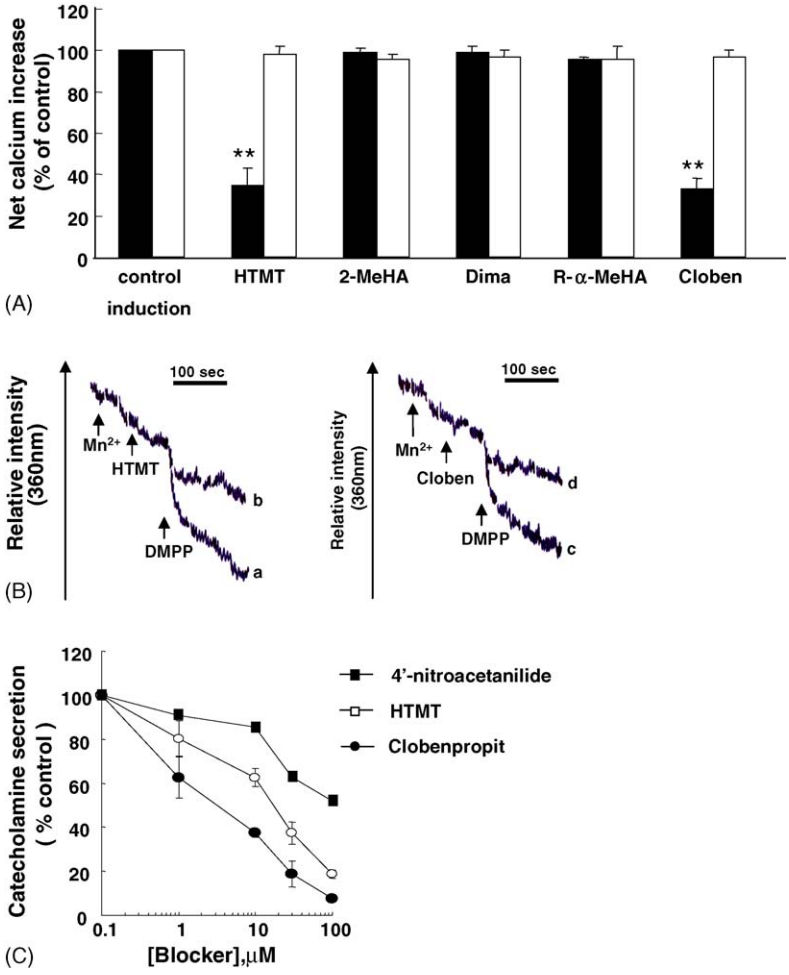

Fig. 10 – Comparison of the effect of HTMT with that of other synthetic histamine receptor agonists. (A) Cells were pretreated with 10 μM HTMT, 2-methylhistamine (2-MeHA), Dimaprit (Dima), R-α-methylhistamine (R-α-MeHA), or clobenpropit (Cloben) for 5 min prior to the addition of 10 μM DMPP (closed bars) or 60 mM KCl (open bars), and $[Ca^{2+}]_i$ was measured. Significant differences between DMPP alone and DMPP + HTMT or DMPP + clobenpropit are presented. $^{**}P < 0.01$. Data are the mean ± S.E.M. (bars) values of triplicate measurements. (B) Bovine chromaffin cells were preloaded with fura-2/AM and Mn^{2+}-induced fura-2 fluorescence quenching was recorded by measuring 10 μM DMPP-induced Mn^{2+} influx in the presence of HTMT (trace a) or clobenpropit (trace c), as described in Section 2. The results are depicted as fluorescence intensities at 360 nm (F_{360}). Traces b and d represent Mn^{2+} influx in the presence of DMPP alone. The data presented are representative of four independent experiments, and the results were reproducible. (C) Effect of 4′-nitroacetanilide, HTMT, and clobenpropit on DMPP-induced CA secretion. Bovine chromaffin cells were pretreated with 4′-nitroacetanilide (closed boxes), HTMT (open circles), or clobenpripit (closed circles) prior to treatment with 10 μM DMPP, and CA secretion was measured by HPLC. Data are the mean ± S.E.M. (bars) values of triplicate measurements.

functional moiety in its interaction with nAChRs. Indeed, we found that the *N*-(4-trifluoromethylphenyl)amide group in histamine-trifluoromethyltoluide inhibits nicotinic receptor-mediated Ca^{2+} influx and CA secretion. According to Fig. 10, clobenpropit showed prominent inhibitiory effect on the nAChR-induced signaling. Clobenpropit is widely known as H3 histamine receptor antagonist [36] and H4 histamine receptor agonist [37]. The structure of clobenpropit is also derived from histamine. Its structure is similar to HTMT in some aspects, but it does not have a *N*-(4-trifluoromethylphenyl)amide moiety. Instead, it has a similar chemical structure, *N*-(*p*-chlorobenzyl)isothiourea group. Both of the structures are capable of inhibitory the nAChR-mediated calcium response, but the results show that the minor difference in the structure has affected the potency. This can be a useful point for further investigation.

We also found that the IC_{50} of histamine-trifluoromethyltoluide on sodium increase was lower than that on calcium, thus explaining why an electrophysiologically higher concentration of antagonist is needed to suppress the activation of VSCCs compared with VSSCs. That is, the concentration of histamine-trifluoromethyltoluide sufficient to inhibit intracellular sodium increase may not inhibit calcium rise. We also found that the histamine-trifluoromethyltoluide inhibition of cytosolic calcium increase is a downstream phenomenon of membrane depolarization caused by the activation of nAChRs,

whereas the other direct pathways that could activate voltage-sensitive calcium channels are not significantly influenced by histamine-trifluoromethyltoluide. Although calcium channels are activated during the activation of nAChRs, both the histamine-trifluoromethyltoluide inhibition of DMPP-induced sodium increase and the absence of an inhibitory effect on high K^+-induced calcium increase indicate that nAChRs, but not calcium channels, are the specific target of histamine-trifluoromethyltoluide.

There are various neuronal nAChRs subtypes, including α4β2 nAChRs, α7 nAChRs, and α3β4* nAChRs [38]. Using subtype specific agonists to determine the subtype specificity of histamine-trifluoromethyltoluide, we found that histamine-trifluoromethyltoluide significantly inhibited the increase in intracellular calcium induced by 5-Iodo-A-85380 and UB165, selective agonists of α4β2 and α3β2, respectively, indicating that histamine-trifluoromethyltoluide is also effective on the subtype selective nAChR agonists. Experiments with a range of nAChR subtypes would be required to conclude that HTMT blocks a broad spectrum of AChR subtypes. However, when we examined the effect of HTMT on the calcium increase evoked by UB-165 and A-85380, which are selective agonists of α4β2 subtype, the calcium increase was also significantly inhibited (Fig. 9A and B). The IC_{50} for each agonists were all similar with the IC_{50} for DMPP. In addition, 30 μM of HTMT completely blocked nAChR subtype agonist-induced calcium increase (Fig. 9B), suggesting that HTMT can be used as a non-subtype specific nAChR antagonist.

CAs are involved in a variety of stressful stimuli. For example, the effects of cold stress [39], ether stress [40], and systemic hypotension [41] at least partly involve an activation of the brainstem NA/EP afferents to the paraventricular nucleus (PVN). The ability of CAs to stimulate the release of corticotropin-releasing hormone (CRH) has also been documented [42]. Nicotine has been shown to stimulate NE release in the PVN in a concentration-dependent manner, which was well correlated with ACTH secretion, regardless of the route of nicotine delivery [43]. Accordingly, the specific effect of histamine-trifluoromethyltoluide on CA secretion through the inhibition of nAChRs activity indicates that histamine-trifluoromethyltoluide could modulate abnormal nerve stimulation during extremely stressful situations. In addition, histamine-trifluoromethyltoluide may be effective as a negative regulator of the HPA axis, although the correlation between its inhibitory effect and the physiological function of histamine-trifluoromethyltoluide has not yet been determined.

Recently, mecamylamine, a noncompetitive and nonselective channel blocker of nAChRs, as well as lobeline, a competitive nicotinic receptor antagonist, have been demonstrated to have utility as tobacco smoking cessation agents [44,45]. Furthermore, preclinical results suggest that lobeline may be a potential treatment for psychostimulant abuse [46]. In addition, we previously reported several other kinds of nAChR antagonists [21,47,48]. We, however, could not find any similarity in the structures of these antagonists as compared with N-(4-trifluoromethylphenyl)amide group of HTMT, indicating the novelty of this study.

In conclusion, our results suggest that histamine-trifluoromethyltoluide represents a promising new candidate compound that may be useful in the search for small-molecule pharmacotherapies for nAChR-related brain diseases. In addition, histamine-trifluoromethyltoluide could be useful tools in the study of nAChR-mediated signal transduction in neuronal systems.

Acknowledgements

We thank Mr. Byung-Soon Kang in Kyung-Buk Packers Company, Inc. (Pohang, South Korea) for kindly providing the bovine adrenal gland. This work was supported by the Frontier Research Project of the POSCO, Brain Korea 21 Program of the Korean Ministry of Education and BioGreen 21 Program of the Korean Rural Development Administration (Code #: 20050401-034-641-190-01-00), and the Brain Neurobiology Research Program (M10412000088-04N1200-08810).

REFERENCES

[1] Perlman RL, Chalfie M. Catecholamine release from the adrenal medulla. Clin Endocrinol Metab 1977;6(3):551–76.
[2] Aunis D. Exocytosis in chromaffin cells of the adrenal medulla. Int Rev Cytol 1998;181:213–320.
[3] Park TJ, Shin SY, Suh BC, Suh EK, Lee IS, Kim YS, et al. Differential inhibition of catecholamine secretion by amitriptyline through blockage of nicotinic receptors, sodium channels, and calcium channels in bovine adrenal chromaffin cells. Synapse 1998;29(3):248–56.
[4] Mannelli M, Pupilli C, Lanzillotti R, Ianni L, Bellini F, Sergio M. Role for endogenous dopamine in modulating sympathetic-adrenal activity in humans. Hypertens Res 1995;18(Suppl. 1):S79–86.
[5] Teschemacher AG. Real-time measurements of noradrenaline release in periphery and central nervous system. Auton Neurosci 2005;117(1):1–8.
[6] Weinberger J. The role of dopamine in cerebral ischemic damage: a review of studies with Gerald Cohen. Parkinsonism Relat Disord 2002;8(6):413–6.
[7] Remy P, Samson Y. The role of dopamine in cognition: evidence from functional imaging studies. Curr Opin Neurol 2003;16(Suppl. 2):S37–41.
[8] Seeman P, Van Tol HH. Dopamine receptor pharmacology. Trends Pharmacol Sci 1994;15(7):264–70.
[9] Gotti C, Clementi F. Neuronal nicotinic receptors: from structure to pathology. Prog Neurobiol 2004;74(6):363–96.
[10] Lamb PW, Melton MA, Yakel JL. Inhibition of neuronal nicotinic acetylcholine receptor channels expressed in Xenopus oocytes by beta-amyloid1–42 peptide. J Mol Neurosci 2005;27(1):13–21.
[11] Armstrong SM, Stuenkel EL. Progesterone regulation of catecholamine secretion from chromaffin cells. Brain Res 2005;1043(1–2):76–86.
[12] Zalat S, Elbana S, Rizzoli S, Schmidt JO, Mellor IR. Modulation of nicotinic acetylcholine and N-methyl-D-aspartate receptors by some Hymenopteran venoms. Toxicon 2005;46(3):282–90.
[13] Gentry CL, Lukas RJ. Local anesthetics noncompetitively inhibit function of four distinct nicotinic acetylcholine receptor subtypes. J Pharmacol Exp Ther 2001;299(3):1038–48.
[14] Hama A, Menzaghi F. Antagonist of nicotinic acetylcholine receptors (nAChR) enhances formalin-induced nociception

in rats: tonic role of nAChRs in the control of pain following injury.. Brain Res 2001;888(1):102–6.
[15] Caban AJ, Hama AT, Lee JW, Sagen J. Enhanced antinociception by nicotinic receptor agonist epibatidine and adrenal medullary transplants in the spinal subarachnoid space. Neuropharmacology 2004;47(1): 106–16.
[16] Khan IM, Stanislaus S, Zhang L, Taylor P, Yaksh TL. A-85380 and epibatidine each interact with disparate spinal nicotinic receptor subtypes to achieve analgesia and nociception. J Pharmacol Exp Ther 2001;297(1):230–9.
[17] Farzin D, Asghari L, Nowrouzi M. Rodent antinociception following acute treatment with different histamine receptor agonists and antagonists. Pharmacol Biochem Behav 2002;72(3):751–60.
[18] Qiu R, Melmon KL, Khan MM. Effects of histamine-trifluoromethyl-toluidide derivative (HTMT) on intracellular calcium in human lymphocytes. J Pharmacol Exp Ther 1990;253(3):1245–52.
[19] Kim DC, Lee SY, Jun DJ, Kim SH, Lee JH, Hur EM, et al. Inhibition of store-operated calcium entry-mediated superoxide generation by histamine trifluoromethyltoluide independent of histamine receptors. Biochem Pharmacol 2005;70(11):1613–22.
[20] Kilpatrick DL, Ledbetter FH, Carson KA, Kirshner AG, Slepetis R, Kirshner N. Stability of bovine adrenal medulla cells in culture. J Neurochem 1980;35(3):679–92.
[21] Woo KC, Park YS, Jun DJ, Lim JO, Baek WY, Suh BS, et al. Phytoestrogen cimicifugoside-mediated inhibition of catecholamine secretion by blocking nicotinic acetylcholine receptor in bovine adrenal chromaffin cells. J Pharmacol Exp Ther 2004;309(2):641–9.
[22] Koh DS, Hille B. Rapid fabrication of plastic-insulated carbon-fiber electrodes for micro-amperometry. J Neurosci Methods 1999;88(1):83–91.
[23] Choi SY, Ha H, Kim KT. Capsaicin inhibits platelet-activating factor-induced cytosolic Ca^{2+} rise and superoxide production. J Immunol 2000;165(7):3992–8.
[24] Friedman JE, Lelkes PI, Lavie E, Rosenheck K, Schneeweiss F, Schneider AS. Membrane potential and catecholamine secretion by bovine adrenal chromaffin cells: use of tetraphenylphosphonium distribution and carbocyanine dye fluorescence. J Neurochem 1985;44(5):1391–402.
[25] Kitayama S, Ohtsuki H, Morita K, Dohi T, Tsujimoto A. Bis-oxonol experiment on plasma membrane potentials of bovine adrenal chromaffin cells: depolarizing stimuli and their possible interaction. Neurosci Lett 1990;116(3):275–9.
[26] Heldman E, Barg J, Vogel Z, Pollard HB, Zimlichman R. Correlation between secretagogue-induced Ca^{2+} influx, intracellular Ca^{2+} levels and secretion of catecholamines in cultured adrenal chromaffin cells. Neurochem Int 1996;28(3):325–34.
[27] Marley PD, Wallace D, Donald A, McKenzie S. How does histamine evoke catecholamine secretion from bovine chromaffin cells? Ann N Y Acad Sci 2002;971:148–9.
[28] Rhoads AR, Parui R, Vu ND, Cadogan R, Wagner PD. ATP-induced secretion in PC12 cells and photoaffinity labeling of receptors. J Neurochem 1993;61(5):1657–66.
[29] Suh BC, Lee CO, Kim KT. Signal flows from two phospholipase C-linked receptors are independent in PC12 cells. J Neurochem 1995;64(3):1071–9.
[30] Hur EM, Park TJ, Kim KT. Coupling of L-type voltage-sensitive calcium channels to P2X(2) purinoceptors in PC-12 cells. Am J Physiol Cell Physiol 2001; 280(5):C1121–9.
[31] Kulak JM, Sum J, Musachio JL, McIntosh JM, Quik M. 5-Iodo-A-85380 binds to alpha-conotoxin MII-sensitive nicotinic acetylcholine receptors (nAChRs) as well as alpha4beta2* subtypes. J Neurochem 2002;81(2):403–6.
[32] Bisson WH, Scapozza L, Westera G, Mu L, Schubiger PA. Ligand selectivity for the acetylcholine binding site of the rat alpha4beta2 and alpha3beta4 nicotinic subtypes investigated by molecular docking. J Med Chem 2005;48(16):5123–30.
[33] Lau WH, Kwan YW, Au AL, Cheung WH. An in vitro study of histamine on the pulmonary artery of the Wistar–Kyoto and spontaneously hypertensive rats. Eur J Pharmacol 2003;470(1–2):45–55.
[34] Qiu R, Melmon KL, Khan MM. Effects of lymphokines and mitogens on a histamine derivative-induced intracellular calcium mobilization and inositol phosphate production. Biochem Pharmacol 1994;47(11):2097–103.
[35] Leurs R, Smit MJ, Timmerman H. Molecular pharmacological aspects of histamine receptors. Pharmacol Ther 1995;66(3):413–63.
[36] Badenhorst HE, Maharaj DS, Malan SF, Daya S, van Dyk S. Histamine-3 receptor antagonists reduce superoxide anion generation and lipid peroxidation in rat brain homogenates. J Pharm Pharmacol 2005;57(6):781–5.
[37] Gutzmer R, Diestel C, Mommert S, Kother B, Stark H, Wittmann M, et al. Histamine H4 receptor stimulation suppresses IL-12p70 production and mediates chemotaxis in human monocyte-derived dendritic cells. J Immunol 2005;174(9):5224–32.
[38] Lukas RJ, Changeux JP, Le Novere N, Albuquerque EX, Balfour DJ, Berg DK, et al., International Union of Pharmacology. XX. Current status of the nomenclature for nicotinic acetylcholine receptors and their subunits. Pharmacol Rev 1999;51(2):397–401.
[39] Pacak K, Armando I, Fukuhara K, Kvetnansky R, Palkovits M, Kopin IJ, et al. Noradrenergic activation in the paraventricular nucleus during acute and chronic immobilization stress in rats: an in vivo microdialysis study. Brain Res 1992;589(1):91–6.
[40] Plotsky PM. Facilitation of immunoreactive corticotropin-releasing factor secretion into the hypophysial-portal circulation after activation of catecholaminergic pathways or central norepinephrine injection. Endocrinology 1987;121(3):924–30.
[41] Van Huysse JW, Bealer SL. Central nervous system norepinephrine release during hypotension and hyperosmolality in conscious rats. Am J Physiol 1991; 260(6 Pt 2):R1071–6.
[42] Tsagarakis S, Holly JM, Rees LH, Besser GM, Grossman A. Acetylcholine and norepinephrine stimulate the release of corticotropin-releasing factor-41 from the rat hypothalamus in vitro. Endocrinology 1988;123(4):1962–9.
[43] Sharp BM, Matta SG. Detection by in vivo microdialysis of nicotine-induced norepinephrine secretion from the hypothalamic paraventricular nucleus of freely moving rats: dose-dependency and desensitisation. Endocrinology 1993;133(1):11–9.
[44] Curzon P, Kim DJ, Decker MW. Effect of nicotine, lobeline, and mecamylamine on sensory gating in the rat. Pharmacol Biochem Behav 1994;49(4):877–82.
[45] Schneider DA, Perrone M, Galligan JJ. Nicotinic acetylcholine receptors at sites of neurotransmitter release to the guinea pig intestinal circular muscle. J Pharmacol Exp Ther 2000;294(1):363–9.
[46] Dwoskin LP, Crooks PA. A novel mechanism of action and potential use for lobeline as a treatment for psychostimulant abuse. Biochem Pharmacol 2002;63(2):89–98.
[47] Park TJ, Park YS, Lee TG, Ha H, Kim KT. Inhibition of acetylcholine-mediated effects by borneol. Biochem Pharmacol 2003;65(1):83–90.
[48] Park TJ, Seo HK, Kang BJ, Kim KT. Noncompetitive inhibition by camphor of nicotinic acetylcholine receptors. Biochem Pharmacol 2001;61(7):787–93.